

1 Dynamic Nuclear Polarization (DNP) in Diamond

Jochen Scheuer^{1,2} and Boris Naydenov^{1,3}

¹Institute for Quantum Optics, Universität Ulm, Albert-Einstein-Allee 11, 89069 Ulm, Germany

²NVision Imaging Technologies GmbH, Albert-Einstein-Allee 11, 89081 Ulm, Germany

³Institute for Nanospectroscopy, Helmholtz-Zentrum Berlin für Materialien und Energie GmbH, Berlin, Germany

Keywords: NV centers in diamond, hyperpolarization, dynamic nuclear polarization (DNP), nuclear magnetic resonance (NMR)

Here we review the recent studies on Dynamic Nuclear Polarization (DNP) using nitrogen-vacancy centers in diamond (NV). First we show the basic principles of DNP and explain its importance for Nuclear Magnetic Resonance (NMR). Then we give an overview of the recently developed DNP methods, which utilize the unique properties of NV centers and demonstrate their advantages compared to conventional DNP techniques. Finally we show the potential applications of diamond based DNP for improving the sensitivity and resolution Magnetic Resonance Imaging (MRI).

1.1 Introduction to DNP

In this chapter the recent progress on Dynamic Nuclear Polarization (DNP or often called hyperpolarization) in diamond will be reviewed. DNP is a rapidly developing field of research and recently diamond found application there. This is due to its color centers and their suitable physical properties. We will begin with a short introduction to Nuclear Magnetic Resonance (NMR) and describe how DNP can improve the NMR signal by several orders of magnitude. Then we will briefly introduce recently demonstrated DNP methods utilizing the negatively charged Nitrogen-Vacancy centers [1] (NVs) for achieving high DNP efficiency.

NMR is probably the most important spectroscopy method with wide application in biology, chemistry and material science [2, 3]. It allows not only to determine the chemical composition and structure of various molecules, proteins and materials, but also to study many dynamical processes like diffusion. Magnetic Resonance Imaging (MRI), which is based on NMR, is an invaluable medical tool, which is applied for diagnosing many forms of diseases as well as different injuries. Both NMR and MRI utilize the absorption of Radio Frequency (RF) radiation by nuclear spins in a static magnetic field, where the local atomic environment can be determined by the shifts of the spin resonance frequency: the chemical shift. The NMR (and correspondingly MRI)

1 Dynamic Nuclear Polarization (DNP) in Diamond

signal strength is proportional to the nuclear spin polarization in thermal equilibrium P_{therm} , which is defined as:

$$P_{\text{therm}} = \frac{N_{\uparrow} - N_{\downarrow}}{N_0} = \tanh\left(\frac{\gamma_n h B_0}{2k_B T}\right) \quad (1.1)$$

where N_{\uparrow} (N_{\downarrow}) is the number of nuclear spins aligned along (opposite) the magnetic field, $N_0 = N_{\uparrow} + N_{\downarrow}$, γ_n is the nuclear spin gyromagnetic ratio, h and k_B are the Plank and Boltzmann constants, T is the temperature, B_0 is the strength of the applied static magnetic field and N_{\uparrow} and N_{\downarrow} are given by:

$$N_{\uparrow} = N_0 \cdot \exp\left(\frac{\gamma_n h B_0}{2k_B T}\right) \quad \text{and} \quad N_{\downarrow} = N_0 \cdot \exp\left(-\frac{\gamma_n h B_0}{2k_B T}\right).$$

If we take for example protons (^1H , nuclear spin $I = 1/2$, gyromagnetic ratio $\gamma_n = 42.576$ MHz/T) at room temperature in a very high magnetic field of $B_0 = 20$ T, we become a polarization of $P_{\text{therm}} = 7 \times 10^{-5} \approx 10^{-4}$. In other words from 10 000 spins, only one will contribute to the NMR signal, the rest of them will be equally aligned along and opposite B_0 , thus canceling their contribution. Obviously this is a serious drawback, since only a small part of the ensemble will give a signal. Moreover, this is an intrinsic property of the spin ensemble and it can be only increased by applying higher magnetic field, although 20 T is already experimentally quite challenging and expensive for routine experiments. Fortunately, in 1953 Albert Overhauser (at that time a graduate student) came with the ingenious idea to utilize the much higher electron spin polarisation [4], which is explained in the following (for a more detailed description see [3], Chapter 7.4). Let us take a single electron spin (e , $S = 1/2$) coupled to a single nuclear spin (n , $I = 1/2$) having Zeeman energies of $\omega_S = \gamma_e B_0$ and $\omega_I = \gamma_n B_0$ with a hyperfine coupling strength A . There will be four possible states n_{\uparrow} , n_{\downarrow} , e_{\uparrow} and e_{\downarrow} , with four allowed transitions. The energy level scheme is shown in figure 1.1.

Overhauser discovered that when both electron spin resonance (ESR) transitions are saturated by applying a strong microwave (MW) field, the electron spin polarisation is transferred to the nuclear spins ensemble. This leads to a higher nuclear spin polarisation P_{DNP} , where the increase can reach:

$$\frac{P_{\text{DNP}}}{P_{\text{therm}}} = \frac{\gamma_e}{\gamma_n}. \quad (1.2)$$

This process is called "Overhauser effect", the maximum ratio for protons is about 670. This enhancement of nuclear spin polarization is known as Dynamic Nuclear Polarisation (DNP) and is widely used in NMR. A wide spread modification of this is the "solid effect", where one of the dipolar forbidden transition $|n_{\uparrow}e_{\uparrow}\rangle \leftrightarrow |n_{\downarrow}e_{\downarrow}\rangle$ or $|n_{\downarrow}e_{\uparrow}\rangle \leftrightarrow |n_{\uparrow}e_{\downarrow}\rangle$ is driven via MW irradiation. During this process there is a transfer of spin polarization from the electron to nuclear spins [5].

The transfer of spin polarization is often called flip-flop process and in the language of quantum mechanics is described by the following Hamiltonian:

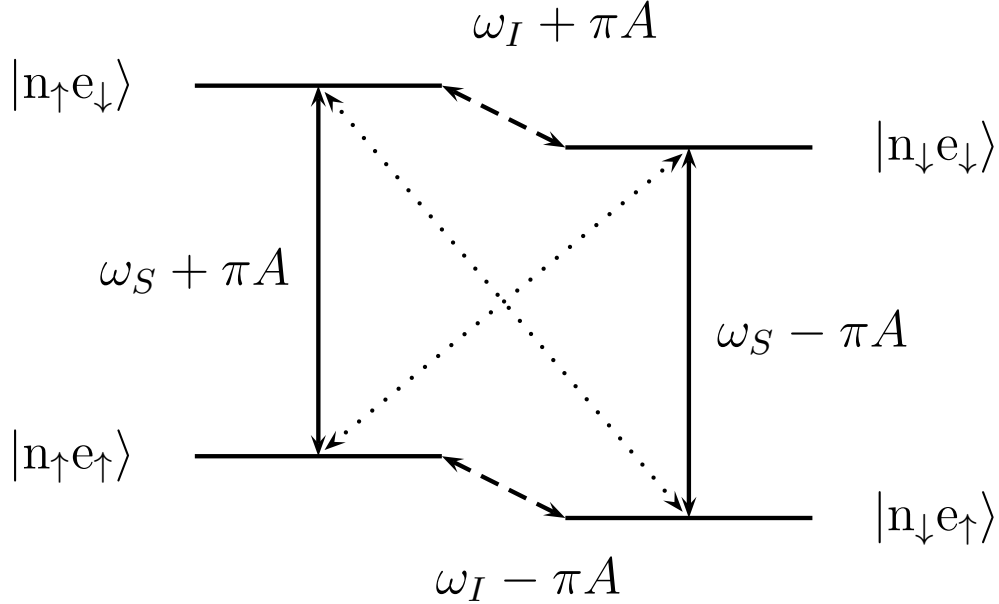


Figure 1.1: An electron spin $S = 1/2$ coupled to a nuclear spins $I = 1/2$. The solid (dashed) lines represent the allowed electron (nuclear) spin transitions, the dotted lines show the forbidden transitions.

$$H_{\text{HF}} = A_{\perp}(S_{+}I_{-} + S_{-}I_{+}), \quad (1.3)$$

where the hyperfine interaction term A_{\perp} is a measure for the rate of polarization transfer. The effect of this Hamiltonian can be shown explicitly, when it acts on the state $|n_{\uparrow}e_{\uparrow}\rangle + |n_{\downarrow}e_{\uparrow}\rangle$ where the electron spin is polarized and the nuclear spin is in a mixed state. It will generate the state $|n_{\downarrow}e_{\uparrow}\rangle + |n_{\downarrow}e_{\downarrow}\rangle$ with the nuclear spin being now polarized and leaving the electron in a mixed state.

The above mentioned ratio 1.2 is valid for thermal electron spin polarization, which is proportional to the applied magnetic field and to the temperature according to equation 1.1. To achieve hyperpolarization often the NMR samples are mixed with stable radicals and then cooled down to several Kelvin and kept in a magnetic field of several Tesla. The sample is then irradiated with a high power MW in order to saturate the ESR transitions and to realize DNP. The transfer of spin polarization is relatively slow (in the order of an hour), due to the long relaxation time T_1 of the electron spins at these

conditions. After polarizing, the sample is quickly warmed up, dissolved in a solvent and can be measure. This DNP method is know as dissolution DNP and has been already applied for MRI [6, 7, 8].

As we have seen the maximum achievable nuclear spin polarization is always limited by the polarization of the used electron spins. However, the latter can reach very high non-equilibrium values (above 0.9) for example in optically generated spin triplet states and for color centers in diamond as we will see later. In this case light illumination of the samples creates electron spin triplets, which are already spin polarized. Then almost any DNP method can be applied to polarize nuclear spins and many orders of magnitude improvement in the NMR signal have been demonstrated [9, 10, 11]. The advantage of this method is not only the very high signal enhancement, but also the ability to continuously polarize the electron spins just by shining light, whereas in conventional DNP (using thermal polarization) the speed of re-polarization is limited by the electron spin T_1 . The disadvantage is the requirement for an optical access and also that the samples have to remain stable under illumination from the high laser power typically used.

1.2 DNP with Nitrogen-Vacancy (NV) Centers in Diamond

Point defect centers in diamond show extraordinary physical properties with various potential applications in the emerging quantum technology (as described in the remaining chapters in this book). The most prominent and well studied color centers are the above mentioned NVs [1]. Due to their strong optical transition from the triplet ground state to the triplet excited state, single NVs can be easily optically observed. Moreover, since the emitted fluorescence depends on the state of the electron spin in the ground state, the electron spin of single NVs can be detected and controlled using MW pulses. These unique properties have been explored to demonstrate that NVs can serve as sensors for magnetic [12, 13, 14] and electric [15] fields, temperature [16] and pressure with very high sensitivity and nano-scale spatial resolution.

The ground state electron spin of the NV can be polarized above 0.92 into the $m_S = 0$ state [17, 18] just by applying a laser pulse of few microseconds length.

1.2.1 All optical DNP techniques

DNP at the level anti-crossing (LAC)

If there is a nuclear spin coupled to an NV center, it would shift only the $m_S = \pm 1$ levels, while leaving the $m_S = 0$ untouched. Since the latter is polarized by laser irradiation, this polarization can be transferred to the nuclear spins only by applying some MW or/and RF pulses. However, there are some conditions, where no RF or MW is required to obtain a very efficient polarization transfer to realize DNP [19]. The dependence of the NV's spin level on a applied magnetic field (along the NV axis defined as z -axis) is shown in figure 1.2. There is an anti-crossing of the levels of the ground state at $B_{GSLAC} = 102.4$ mT and of the excited state around $B_{EXLAC} = 50$ mT,

1.2 DNP with Nitrogen-Vacancy (NV) Centers in Diamond

leading a mixing of the electron spin states $m_S = 0$ and $m_S = -1$. This "turns on" an interaction between the $m_S = 0$ state and the nuclear spin, allowing to realize flip-flop processes (see equation 1.3). This DNP mechanism has been first demonstrated by polarizing the intrinsic ^{15}N nuclear spin of a single NV center above 98 % [19] at $B_{EXLAC} = 500$ mT. The same technique was latter used to polarize an ensemble of ^{13}C nuclear spins in a macroscopic diamond [20, 21]. In the latter experiment the sample was kept at $B_{EXLAC} = 500$ mT for a certain time and then it was shuttled to a high field magnet where the NMR signal was measured, see figure 1.2b. Later studies revealed, that more complex multi-spin processes are involved [22, 23].

The level anti-crossing of the ground state state has been used, to our knowledge, only with a single NV for DNP and nano scale NMR [24, 25].

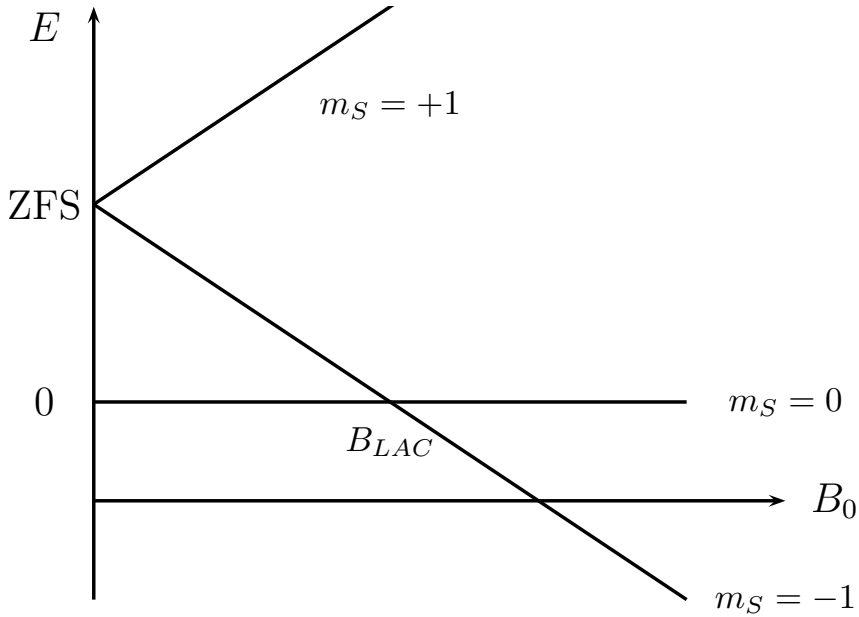


Figure 1.2: Magnetic field dependence of the NV's electron spin levels. The zero field splitting (ZFS, denoted as) is $D_{GS} = 2.87$ GHz and $D_{ES} = 1.4$ GHz for the ground and excited states. Around $B_{GSLAC} = 102.4$ mT and $B_{EXLAC} = 500$ mT there is a mixing of the $m_S = 0$ and $m_S = \pm 1$ states, which is utilized to polarize nuclear spins in the vicinity. See for example [19].

1.2.2 DNP Techniques involving MW and RF irradiation

All-optical DNP methods have the advantage, that no MW or RF irradiation is required, which simplifies the experimental realization. However, as described above, these techniques function only at particular values of the static magnetic field. Another important

requirement is that the field has to be precisely aligned (better than 0.5°), leading to a limited application. Thus more general DNP methods are required, which can be applied at various conditions.

One straightforward realization of DNP is to use the solid effect, since the experiment requires only continuous wave (CW) for both the laser and MW irradiation. This has been demonstrated using a macroscopic diamond with a natural abundance of ^{13}C nuclear spins with an NV concentration of about $1 \times 10^{18} \text{ cm}^{-3}$ [26]. In this experiment the DNP and NMR detection were performed at the same experimental set-up using separate coils for MW and RF excitation. This has the advantage, that the NMR signal is measured immediately after the hyperpolarisation without shuttling the sample, thus allowing to accurately determine the achieved polarization enhancement. The same group reported later [27] the hyperpolarization of ^{13}C enriched diamonds using a similar experimental set-up.

1.2.3 Nuclear spin orientation via electron spin locking (NOVEL) and integrated solid effect (ISE)

The solid effect and its variations are examples of non-coherent DNP methods, where the coherence time of the electron spins does not play a role for the polarization transfer. A more sophisticated control over the spins can be achieved by using MW and RF pulses, thus leading to interesting physical phenomena and to a more efficient polarization transfer at high magnetic fields. This is due to the fact, that the DNP efficiency of the solid effect scale as $\approx 1/B_0$ [28]. The first example of these coherent DNP techniques is the Nuclear spin Orientation via Electron spin Locking (NOVEL) first reported in [29]. The pulse sequence is depicted in figure 1.3a.

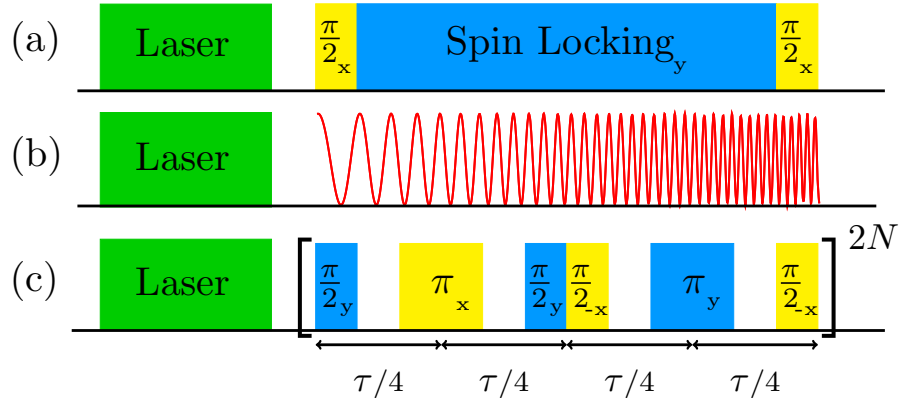


Figure 1.3: Pulse sequences for DNP - NOVEL (a), ISE (b) and PulsePol (c).

The electron spin transition is driven by the spin locking pulse sequence, starting with a $\pi/2$ pulse followed by a long MW pulse, which frequency is shifted by 90° . As long as this pulse is on, the electron spin is in the so-called "dressed state", where the energy levels are shifted by $\hbar\Omega$ with $\Omega = \gamma_e B_1$ (often denoted as ω_1) and B_1 is the

magnetic field amplitude of the applied MW [30]. In order to transfer polarization from the electron to the nuclear spin (polarizing the latter in the n_{\uparrow} state) the Hartmann-Hahn condition [31] $\Omega = \omega_I$ has to be fulfilled, when a flip-flop Hamiltonian becomes active (see equation 1.3). If the phase is shifted by 270° , then the nuclear spin polarized in the n_{\downarrow} state.

NOVEL DNP has been reported for ^{13}C nuclear spins in diamond by using the electron spins of substitutional nitrogen (electron spin $S = 1/2$, P1 centers) [32]. This method has been demonstrated on a single NV in diamond with natural abundance of ^{13}C nuclear spins [33]. In this experiment NMR signal could not be directly measured, but an increased nuclear spin polarization has been indirectly detected. First a laser pulse is applied to polarize the NV center in the $m_S = 0$ state, followed by electron spin-locking for transferring the polarization to one of the surrounding nuclear spins. This pulse sequence is repeated multiple times, leading to a polarization of the surrounding nuclear spins. The latter effect was so strong, that it caused a narrowing of the NV's electron spin line width by a factor of five [33]. However, to observe this phenomenon, strongly coupled nuclear spins with a high polarization are required. Later on the NOVEL technique was implemented for polarizing the ^{13}C nuclear spins in a macroscopic diamond [34]. In this work the maximum reported enhancement of the NMR signal was about 50, probably due to the relatively long transfer time of the sample of about a minute. The diamond was polarized in a conventional electron paramagnetic resonance (EPR) spectrometer and moved to a NMR spectrometer, which was a few hundred meters away. Astonishingly, a DNP effect could be still observed, though with not very high enhancement factor due to the nuclear spin relaxation during the transfer of the sample. Experiments with single NVs suggest [35] that NOVEL is the best DNP technique, compared to the rest discussed in this chapter and serves as a benchmark (see below). NOVEL was the method of choice for attempting to polarize proton nuclear spins on the diamond surface [36, 37] using a single shallow NV center. In these studies no direct evidence of hyperpolarization was reported, but a loss of polarization from the NV's electron spin to the protons was observed.

The NOVEL method is very efficient, as the time to transfer the spin polarization is short, compared to other DNP techniques [38]. However, it has a significant disadvantage. If the electron spin spectrum is very broad, then the Hartmann-Hahn condition cannot be fulfilled since it is sensitive to Ω . More precisely, when the excitation is away from resonance by δ then the effective Rabi frequency is $\Omega_{\text{eff}} = \sqrt{\Omega^2 + \delta^2}$ and the flip-flop process is not efficient any more. Such a situation arises for example for NVs in nanocrystalline diamonds (nanodiamonds or NDs) where a large line broadening occurs due to the random orientation of each crystal. In this case a broadband DNP method as the Integrated Solid Effect (ISE) has to be used [39, 40]. In ISE only a single MW pulse is applied, where the frequency is swept through resonance (see figure 1.3b). Despite the simplicity, there are several parameters, which have to be tuned in order to achieve DNP - sweep range $\Delta\nu$, sweep rate $\dot{\nu} = d\nu/dt$ and the effective Rabi frequency Ω_{eff} . $\Delta\nu$ has to be much larger than the EPR line width in order to cover all possible hyperfine coupling strengths. For $\dot{\nu}$ we have $\dot{\nu} \ll \Omega_{\text{eff}}$ and at the same time the latter should be close to the Hartmann-Hahn condition. During the sweep over the EPR resonance a

Landau-Zener type of transition is realized, leading to a flip-flop process [40]. ISE has been successfully implemented in a macroscopic diamond [34], though the enhancement of the NMR signal was not as good as with NOVEL. This was attributed to the limited bandwidth of the MW resonator, leading to a varying Ω_{eff} at different MW frequencies. For a narrow line width ISE shows about 68 % of the efficiency of NOVEL [35], in this case the latter will be preferred as it is easier to implement experimentally.

A similar DNP method using frequency sweeps at low magnetic fields (10 to 30 mT) was proposed for polarizing ^{13}C nuclear spins in nanodiamond samples with random orientations of the NV centers [41]. This technique was implemented on diamond powders [42, 43] and later used to characterize nanodiamonds via relaxometry [44].

An interesting approach to overcome the line broadening of the NV's electron spin lines is to excite the double quantum transition (DQT) $m_S = -1 \leftrightarrow m_S = +1$ (see figure 1.2) [40, 35]. In conventional experiments of the single quantum transitions $m_S = -1 \leftrightarrow m_S = 0$ or $m_S = 0 \leftrightarrow m_S = +1$ is driven, since is allowed according to the selection rules. However, its transition frequency is much more sensitive to the angle between the magnetic field B_0 and the NV crystal axis. The shift of DQT frequency is smaller compared to SQT and this effect is more prominent at high magnetic fields ($B_0 > 1$ T). Another advantage of DQT is that its associated magnetic dipolar moment is twice larger compared to the SQT, thus increasing the effective hyperfine coupling (A_{\perp}) by a factor of two. DNP of ^{13}C nuclear spins in diamond utilizing the DQT has been demonstrated using single NV centers in diamond [35]. The disadvantage of DQT is that a more complex pulse sequences have to be applied and that a very broad band MW equipment is required.

1.2.4 Pulsed polarization (PulsePol)

The above described DNP methods use either continuous MW irradiation or very long pulses for NOVEL or ISE, where the Hartmann-Hahn condition has to be met. This becomes difficult to implement at high magnetic fields since very fast Rabi frequencies are required, for example at $B_0 = 2$ T $\Omega = 84$ MHz would be needed for protons. Recently another type of DNP method based on short MW pulses was developed for these conditions, instead of continuous driving and is called Pulsed Polarization (PulsePol) [38]. The NOVEL sequence is very efficient but works only in a narrow frequency range and the ISE sequence is broadband but its efficiency is inferior. The PulsePol sequence combines a high polarization efficiency with a broad bandwidth. A flip-process is realized by properly defining the time spacing between the pulses and at first glance Ω does not play a significant role here (see figure 1.3c). However, the higher the magnetic field the shorter become both the time delays and the pulses, leading to higher Rabi frequency. Nevertheless in pulsed experiments it is easier to keep high Ω , compared to CW methods. Furthermore, PulsePol with its broadband pulses is robust and efficient, since the timing τ is experimentally easier to control as the MW power. The effective Hamiltonian is very similar to equation 1.3, differing only by a prefactor:

$$H_{\text{PP}} = \frac{2A_{\perp}}{k\pi} (2 + \sqrt{2}) (S_+I_- + S_-I_+), \quad (1.4)$$

where k is an odd number greater than 1. The condition for achieving polarization transfer is [38]:

$$\tau = \frac{k\pi}{\omega_I} \quad (1.5)$$

where k takes values $k = 3, 5, 11, 13, \dots$ for highest efficiency. This DNP technique has been implemented in single NV centers in diamond [38]. A version of PulsePol based on the modified dynamical decoupling pulses sequence CPMG (Carr Purcell Meiboom Gill [45, 46, 47]) has been reported recently [48].

1.2.5 Nanoscale NMR and Benchmarking DNP with Polarization Readout via Polarization Inversion (PROPI)

DNP methods can be implemented and tested by hyperpolarizing a nuclear spin ensemble and measuring it in a NMR spectrometer. By comparing the NMR signal as a function of the experimental parameters and the applied DNP technique, the best DNP protocol can be chosen. However, this procedure is difficult to implement when a small number of nuclear spins (up to few hundred) are polarized via a single NV center in their vicinity. The very low magnetization of this nano-ensemble cannot be directly measured via a conventional NMR coil, but can only be detected using the same NV center. This is the main idea of the Polarization Readout via Polarization Inversion (PROPI) method [35], schematically shown in figure 1.4.

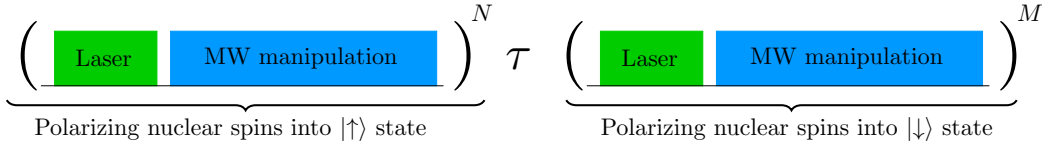


Figure 1.4: Scheme of the Polarization Readout via Polarization Inversion (PROPI) method for performing NMR spectroscopy of nano-scale nuclear spin ensembles. See text for more details.

It consists of two parts, both beginning with a laser pulse to polarize the NV center in the $m_S = 0$ state. The MW pulses in the first part polarize a nuclear spin in the vicinity of the NV into the n_{\uparrow} state. This block (with the laser pulse) is repeated N times until no polarization transfer from the NV to the surrounding nuclear spins is observed. After a delay time τ the second block is repeated M times, where the nuclear spin polarization is inverted (the spins are polarized in the n_{\downarrow} state). With the laser pulses in both parts the NV's electron spin state is read out, allowing to precisely determine how much "spin information" (or spin "quanta" [35]) is transferred to the nuclear spins. The "spin quanta" are summed up during the first and second part of the sequences giving two signal S_N and S_M . Usually when $N = M$ the same "amount" of polarization is induced, leading to $S_N = S_M$ for $\tau = 0$. However, if the MW manipulation is not the same in the different pulse blocks then $S_N \neq S_M$, allowing to compare the performance of DNP techniques pairwise, see [35, 38]. An example of benchmarking DNP is shown

in figure 1.5.

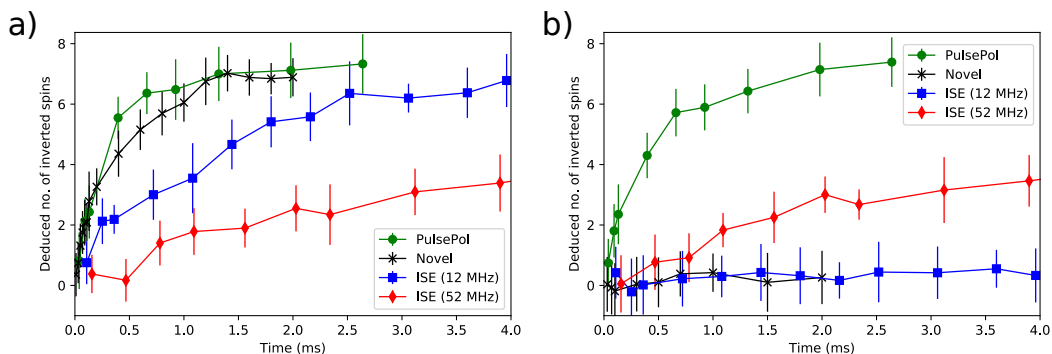


Figure 1.5: Comparing the DNP performance of NOVEL, ISE and PulsePol for resonant (a) and off-resonant excitation (b). 12 and 52 MHz are the corresponding bandwidths of the ISE experiment, where the former is faster, but narrow band, while the latter is slower, but broadband. See [38] for more details.

There is another important application of PROPI. If the same DNP method is used in both pulse blocks (with $N = M$), but the time delay τ between them is increased, then the nuclear spins will start to evolve from the n_{\uparrow} state towards thermal equilibrium. This will result in $S_N \neq S_M$ and by analyzing the time dependence of the signal, the spin-lattice relaxation time T_1 of the nuclear spin ensemble around the electron spin (here an NV center) can be determined. This has been demonstrated in a thin (few atoms thick) layer of ^{13}C spins in the vicinity of a single NV center [49]. Moreover, by applying RF pulses to drive the nuclear spins during the time τ , nano-scale NMR spectroscopy can be realized [49].

1.3 Conclusions and Outlook

We have reviewed here the current status of DNP research using NV centers in diamond. We tried to give an overview over the existing methods and to explain the physical processes involved. One of the remaining challenges is the hyperpolarization of NDs (size below 20 nm), where despite of the recent progress a successful demonstration of DNP with NVs in NDs is still lacking. The main reason for this are the short NV relaxation and coherence times as well as the fast nuclear spin relaxation in those nano-crystals [50]. Once this is realized, NDs with chemically tuned surface can be used as nano-markers for studying bio-chemical processes in cells and small animals [51]. However, although diamond itself is not toxic, NDs could still be harmful for large animals and humans. For this reason many research group are working on the hyperpolarization of nuclear spins in molecules outside of the diamond using NV centers few nanometers below the surface. The goal is DNP on macroscopic samples, metabolites or other physiologically relevant molecules, which can be hyperpolarized and then imaged in a human body with a conventional MRI. This research is motivated by recent reports on metabolic diagnostics

which combines MRI with dissolution DNP. An example for metabolic diagnostics is the discovery of a tumor only after examination of MRI with hyperpolarized pyruvate [6], or the grading of a tumor's stage via spectroscopic analysis of hyperpolarized MRI [52]. An important feature of MRI improved by DNP is not only the increased signal, leading to a higher sensitivity, but also the possibility for selective imaging of particular metabolites differentiating them by their chemical shift. A diamond "hyperpolarizer" has the advantage, that it would require neither low temperatures nor high magnetic field, which will significantly reduce its cost.

Bibliography

- [1] M. W. Doherty et al. The nitrogen-vacancy colour centre in diamond. *Physics Reports*, 528:1–45, 2013.
- [2] M. H. Levitt. *Spin dynamics: basics of nuclear magnetic resonance*. John Wiley & Sons, 2001.
- [3] C. P. Slichter. *Principles of Magnetic Resonance (Springer Series in Solid-State Sciences)*. Springer, 3 edition, 1996.
- [4] A. W. Overhauser. Polarization of nuclei in metals. *Physical Review*, 92(2):411, 1953.
- [5] W. T. Wenckebach. The solid effect. *Applied Magnetic Resonance*, 34(3-4):227, 2008.
- [6] S. J. Nelson et al. Metabolic imaging of patients with prostate cancer using hyperpolarized [1-¹³C]pyruvate. *Science Translational Medicine*, 5:198ra108, 2013.
- [7] S. J. DeVience et al. Metabolic imaging of energy metabolism in traumatic brain injury using hyperpolarized [1-¹³C] pyruvate. *Scientific reports*, 7(1):1907, 2017.
- [8] Z. J. Wang et al. Hyperpolarized ¹³C mri: State of the art and future directions. *Radiology*, 2019.
- [9] J. H. Ardenkjær-Larsen et al. Increase in signal-to-noise ratio of $\sim 10,000$ times in liquid-state nmr. *Proceedings of the National Academy of Sciences*, 100(18):10158–10163, 2003.
- [10] K. Tateishi et al. Room temperature hyperpolarization of nuclear spins in bulk. *Proceedings of the National Academy of Sciences*, 111(21):7527–7530, 2014.
- [11] T. Eichhorn et al. Proton polarization above 70% by dnp using photo-excited triplet states, a first step towards a broadband neutron spin filter. *Nuclear Instruments and Methods in Physics Research Section A: Accelerators, Spectrometers, Detectors and Associated Equipment*, 754:10–14, 2014.
- [12] G. Balasubramanian et al. Nanoscale imaging magnetometry with diamond spins under ambient conditions. *Nature*, 455:648–651, 2008.
- [13] J. R. Maze et al. Nanoscale magnetic sensing with an individual electronic spin in diamond. *Nature*, 455:644–648, 2008.

Bibliography

- [14] L. Rondin et al. Magnetometry with nitrogen-vacancy defects in diamond. *Reports on Progress in Physics*, 77:056503, 2014.
- [15] F. Dolde et al. Electric-field sensing using single diamond spins. *Nature Physics*, 7:459–463, 2011.
- [16] G. Kucsko et al. Nanometre-scale thermometry in a living cell. *Nature*, 500:54–58, 2013.
- [17] J. Harrison et al. Optical spin polarisation of the n-v centre in diamond. *Journal of Luminescence*, 107:245–248, 2004.
- [18] G. Waldherr et al. Dark states of single nitrogen-vacancy centers in diamond unraveled by single shot nmr. *Physical review letters*, 106(15):157601, 2011.
- [19] V. Jacques et al. Dynamic polarization of single nuclear spins by optical pumping of nitrogen-vacancy color centers in diamond at room temperature. *Physical Review Letters*, 102:057403, 2009.
- [20] R. Fischer et al. Optical polarization of nuclear ensembles in diamond. *Physical Review B*, 87:125207, 2013.
- [21] R. Fischer et al. Bulk nuclear polarization enhanced at room temperature by optical pumping. *Physical Review Letters*, 111:057601, 2013.
- [22] R. Wunderlich et al. Optically induced cross relaxation via nitrogen-related defects for bulk diamond ^{13}C hyperpolarization. *Phys. Rev. B*, 96:220407, Dec 2017.
- [23] D. Pagliero et al. Multispin-assisted optical pumping of bulk ^{13}C nuclear spin polarization in diamond. *Phys. Rev. B*, 97:024422, Jan 2018.
- [24] J. D. Wood et al. Quantum probe hyperpolarisation of molecular nuclear spins. *Nature communications*, 8:15950, 2017.
- [25] D. A. Broadway et al. Quantum probe hyperpolarisation of molecular nuclear spins. *Nature communications*, 9(1):1246, 2018.
- [26] J. P. King et al. Room-temperature in situ nuclear spin hyperpolarization from optically-pumped nitrogen vacancy centers in diamond. *Nature Communications*, 6:8965, 2015.
- [27] A. J. Parker et al. Optically pumped dynamic nuclear hyperpolarization in ^{13}C -enriched diamond. *Phys. Rev. B*, 100:041203, 2019.
- [28] G. Mathies et al. Pulsed dynamic nuclear polarization with trityl radicals. *The Journal of Physical Chemistry Letters*, 7:111–116, 2016.
- [29] A. Henstra et al. Nuclear spin orientation via electron spin locking (NOVEL). *Journal of Magnetic Resonance (1969)*, 77(2):389–393, April 1988.

- [30] J.-M. Cai et al. Robust dynamical decoupling with concatenated continuous driving. *New Journal of Physics*, 14:113023, 2012.
- [31] S. R. Hartmann and E. L. Hahn. Nuclear double resonance in the rotating frame. *Physical Review*, 128:2042–2053, 1962.
- [32] E. C. Reynhardt and G. L. High. Dynamic nuclear polarization of diamond. i. nuclear orientation via electron spin-locking. *The Journal of chemical physics*, 109(10):4100, 1998.
- [33] P. London et al. Detecting and polarizing nuclear spins with double resonance on a single electron spin. *Physical Review Letters*, 111:067601, 2013.
- [34] J. Scheuer et al. Optically induced dynamic nuclear spin polarisation in diamond. *New Journal of Physics*, 18:013040, 2016.
- [35] J. Scheuer et al. Robust techniques for polarization and detection of nuclear spin ensembles. *Physical Review B*, 96(17):174436, November 2017.
- [36] P. Fernández-Acebal et al. Toward hyperpolarization of oil molecules via single nitrogen vacancy centers in diamond. *Nano letters*, 18(3):1882–1887, 2018.
- [37] F. Shagieva et al. Microwave-Assisted Cross-Polarization of Nuclear Spin Ensembles from Optically Pumped Nitrogen-Vacancy Centers in Diamond. *NANO LETTERS*, 18:3731–3737, 2018.
- [38] I. Schwartz et al. Robust optical polarization of nuclear spin baths using hamiltonian engineering of nitrogen-vacancy center quantum dynamics. *Science advances*, 4(8):eaat8978, 2018.
- [39] A. Henstra et al. Enhanced dynamic nuclear polarization by the integrated solid effect. *Physics Letters A*, 134(2):134–136, 1988.
- [40] Q. Chen et al. Optical hyperpolarization of ^{13}C nuclear spins in nanodiamond ensembles. *Physical Review B*, 92:184420, 2015.
- [41] P. R. Zangara et al. Dynamics of frequency-swept nuclear spin optical pumping in powdered diamond at low magnetic fields. *Proceedings of the National Academy of Sciences*, 116(7):2512–2520, 2019.
- [42] A. Ajoy et al. Enhanced dynamic nuclear polarization via swept microwave frequency combs. *Proceedings of the National Academy of Sciences*, 115(42):10576–10581, October 2018.
- [43] A. Ajoy et al. Orientation-independent room temperature optical ^{13}C hyperpolarization in powdered diamond. *Science Advances*, 4(5):eaar5492, 2018.
- [44] A. Ajoy et al. Hyperpolarized relaxometry based nuclear t_1 noise spectroscopy in hybrid diamond quantum registers. *arXiv preprint arXiv:1902.06204*, 2019.

Bibliography

- [45] H. Y. Carr and E. M. Purcell. *Phys. Rev.*, 94:630, 1956.
- [46] S. Meiboom and D. Gill. *Rev. Sci. Instrum.*, 29:688, 1958.
- [47] B. Naydenov et al. Dynamical decoupling of a single electron spin at room temperature. *Phys. Rev. B*, 83:081201, 2011.
- [48] J. Lang et al. Quantum bath control with nuclear spin state selectivity via pulse-adjusted dynamical decoupling. *arXiv preprint arXiv:1904.00893*, 2019.
- [49] T. Unden et al. Coherent control of solid state nuclear spin nano-ensembles. *npj Quantum Information*, 4, 2018.
- [50] A. M. Panich et al. Size dependence of ^{13}C nuclear spin-lattice relaxation in micro- and nanodiamonds. *J. Phys.: Condens. Matter*, 27(7):072203, 2015.
- [51] Y. Wu et al. Diamond Quantum Devices in Biology. *ANGEWANDTE CHEMIE-INTERNATIONAL EDITION*, 55(23):6586–6598, 2016.
- [52] M. J. Albers et al. Hyperpolarized ^{13}C lactate, pyruvate, and alanine: noninvasive biomarkers for prostate cancer detection and grading. *Cancer research*, 68(20):8607–8615, 2008.